ADVANCED MATERIALS

Supporting Information

for *Adv. Mater.,* DOI: 10.1002/adma.202106229

Facet-Dependent Surface Charge and Hydration of Semiconducting Nanoparticles at Variable pH

*Shaoqiang Su, Igor Siretanu, Dirkvan den Ende, Bastian Mei, Guido Mul, and Frieder Mugele**

Supplementary Information

Facet-dependent surface charge and hydration of semiconducting nanoparticles at variable pH

Shaoqiang Su[1], Igor Siretanu[1], Dirk van den Ende[1], Bastian Mei[2], Guido Mul[2], Frieder Mugele[1]

[1]Physics of Complex Fluids Group and MESA+ Institute, Faculty of Science and Technology, University of Twente, P.O. Box 217, 7500 AE Enschede, The Netherlands.

[2]Photocatalytic Synthesis Group and MESA+ Institute, Faculty of Science and Technology, University of Twente, P.O. Box 217, 7500 AE Enschede, The Netherlands.

* corresponding author's email: f.mugele@utwente.nl

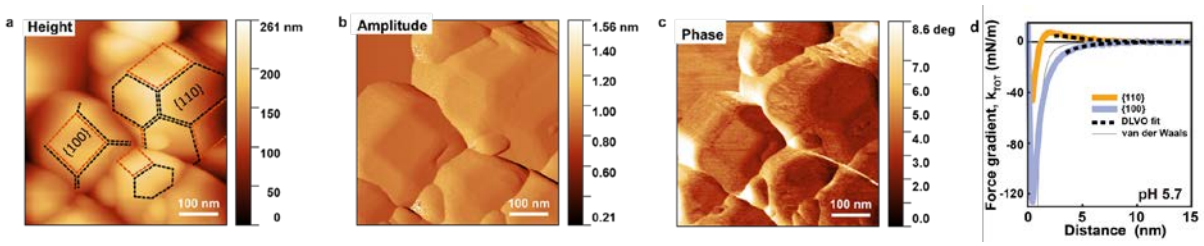

Figure S1. AFM images of $SrTiO_3$ nanoparticles in 10 mM NaCl, pH 5.7. a) Height; b) Amplitude; c) Phase. These images correspond to the location where two dimension (2D) force map measurement shown in Fig. 1c is performed. d) Average total force gradient vs. distance curves across a flat region at the centre of {100} and {110} facets of $SrTiO_3$ particles (marked with black and red circles on the 2D maps in Figure 1b).

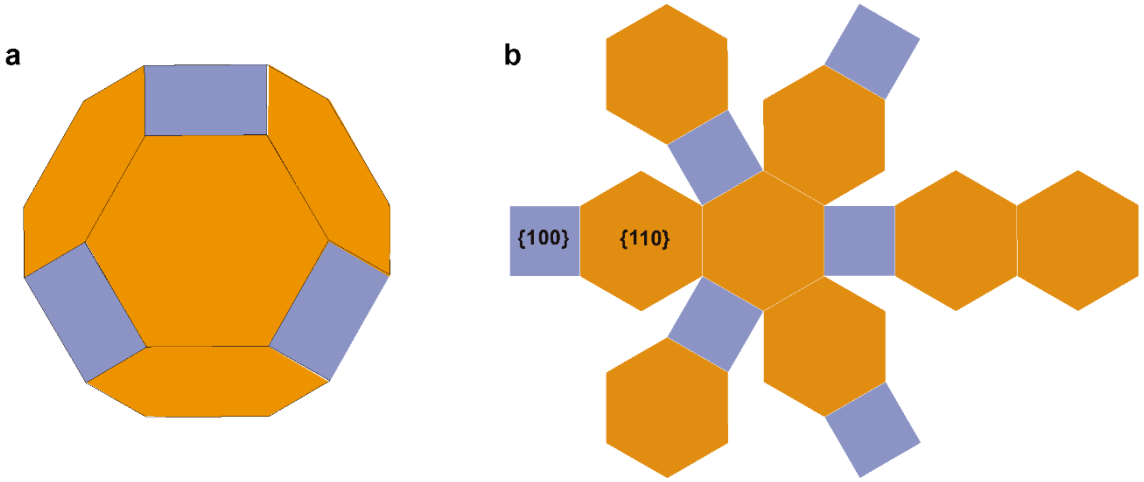

Figure S2. Folded and unfolded sketch of truncated rhombic dodecahedral shape. The facet fraction ratio of {100} shown in blue and {110} shown in orange region is 100:110=0.224:0.776.

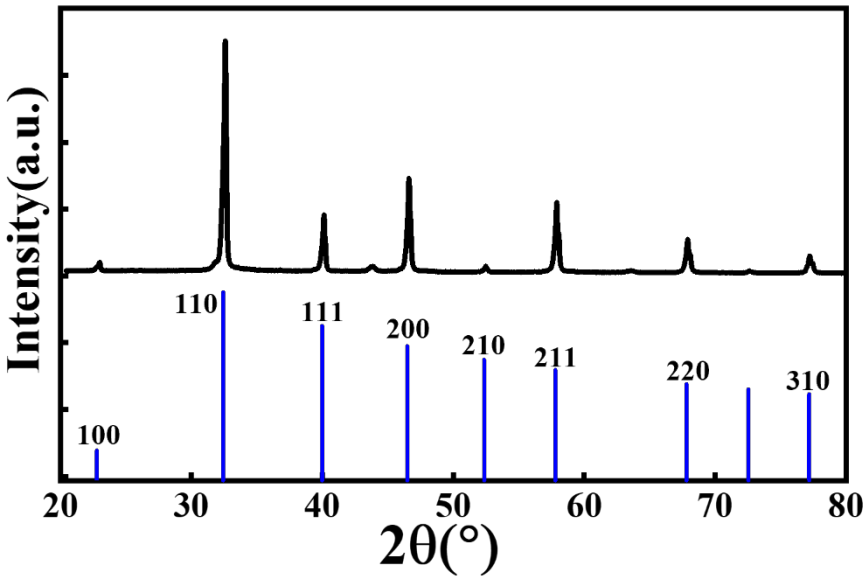

Figure S3. X-ray diffraction (XRD) patterns of hydrothermal synthesized $SrTiO_3$ nanoparticles. Black curve is the XRD patterns of synthesized $SrTiO_3$ nanoparticles. The mesuremets are performed using Bruker D2 Powder XRD. Blue lines correspond to standard PDF card of $SrTiO_3$ (JCPDS No.35-0734).

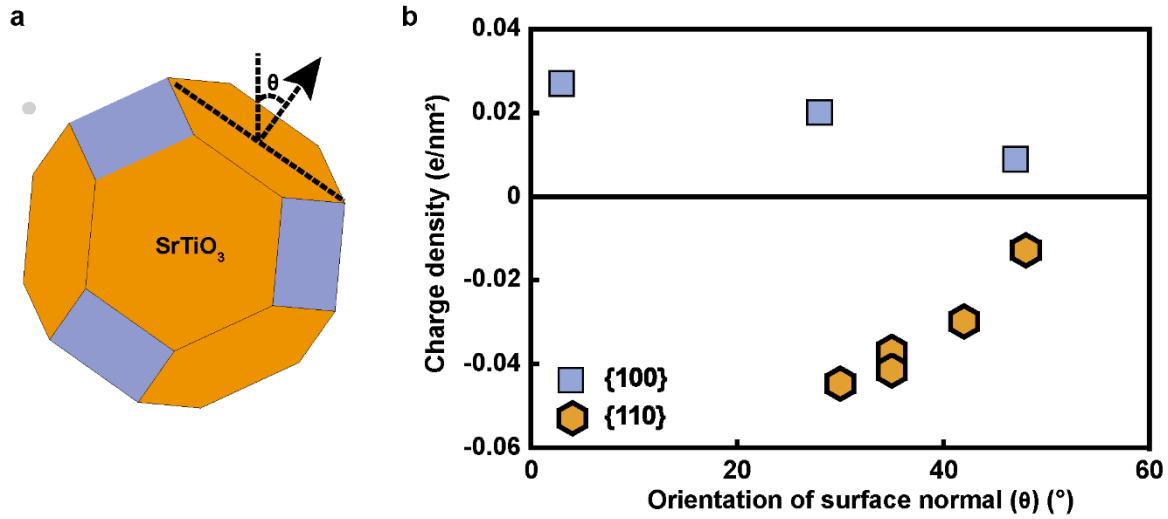

Figure S4. Effect of facet orientation on the surface charge density. a) A sketch representing the orientation of surface normal of {110} facet of $SrTiO_3$. b)The facet orientation effect on the surface charge densities. The surface charge densities were calculated from the local average forces on different facets in Figure 1c.

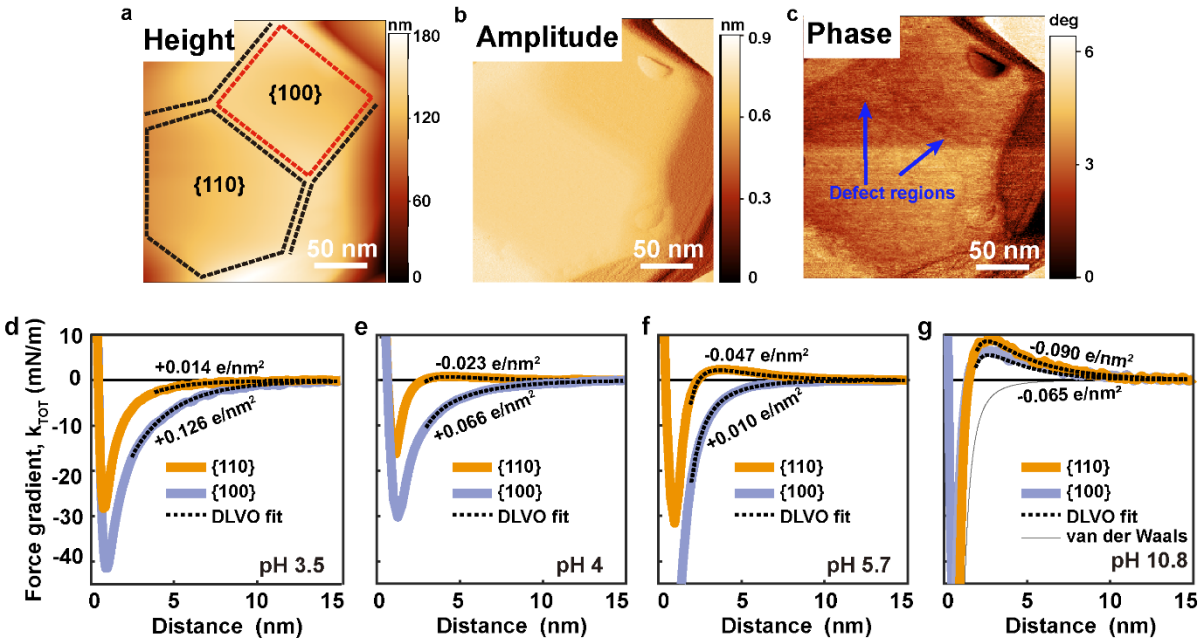

Figure S5. AFM images of $SrTiO_3$ nanoparticle a) Height; b) Amplitude; c) Phase images corresponding to the to the force maps in Figure 2. d-g) Total force gradient vs distance per facet averaged across a flat region at the centre of {100} and {110} facets of $SrTiO_3$ particles (marked with white circles on the 2D maps in Figure 2 a-d).

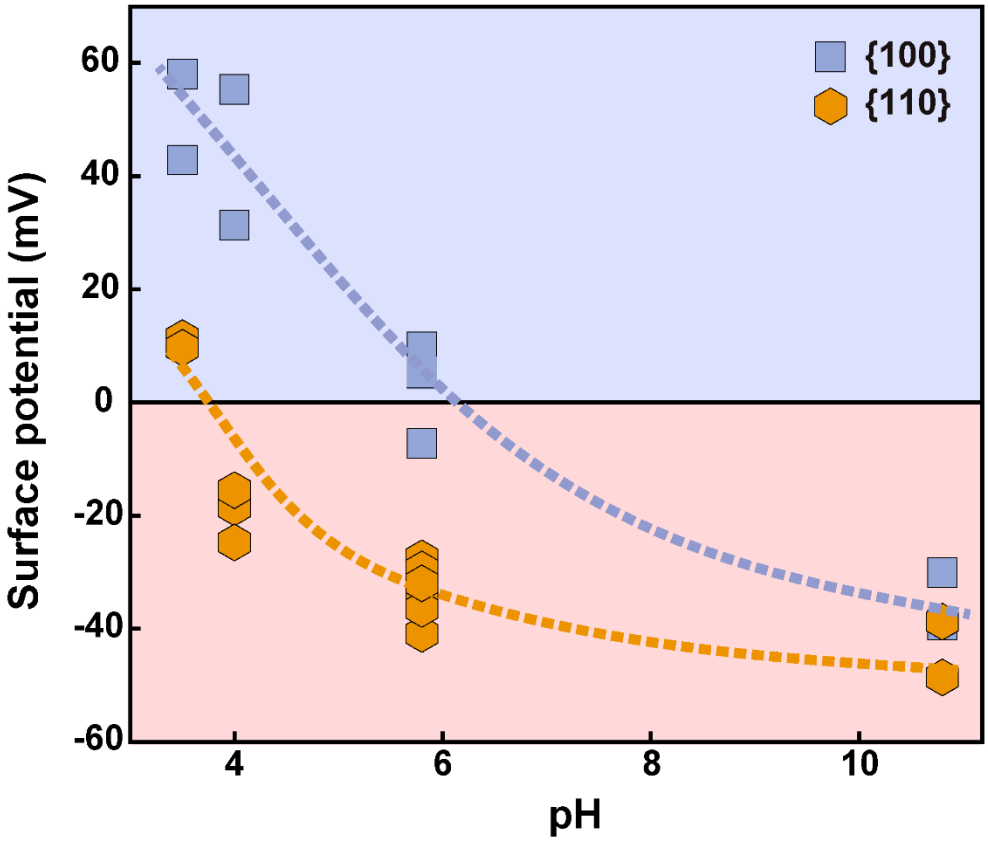

Figure S6. Electrical (potential) properties of {100} and {110} facets $SrTiO_3$ nanoparticles. Surface potential of {100} and {110} facets of $SrTiO_3$ nanoparticle as a function of pH for 10 mM NaCl. The surface charge densities shown in Fig. 3a are converted into surface potentials using the Graham equation (dash lines are guide the eyes).

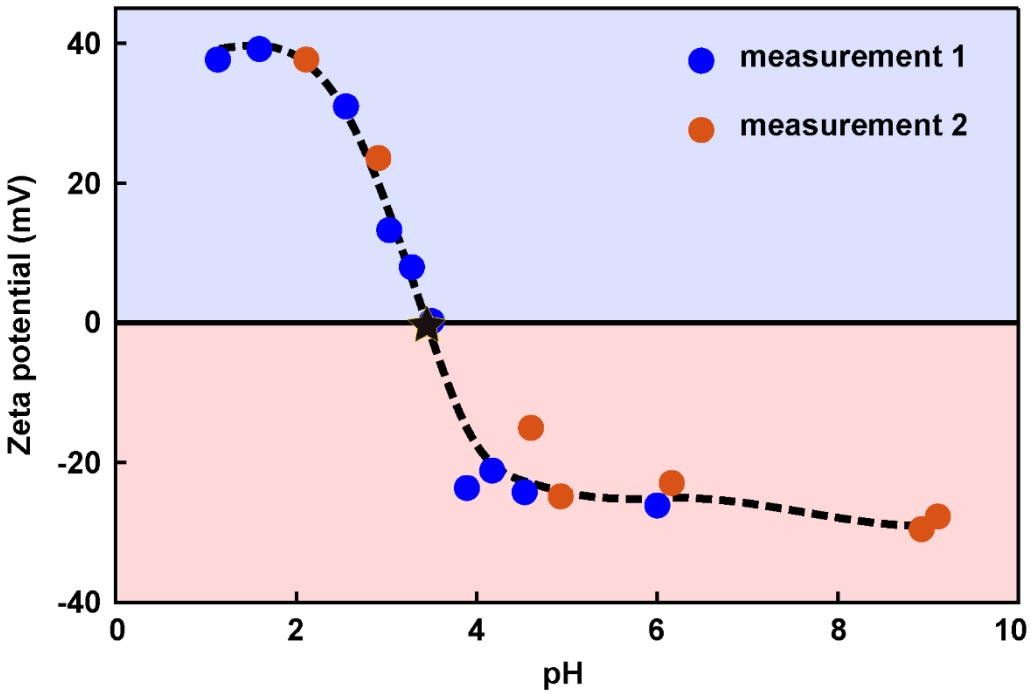

Figure S7. Measured zeta potential of $SrTiO_3$ nanoparticle suspension as function of pH in 10 mM NaCl. Blue and red dots represent two separate measurements (black dash line is to guide the eyes). The isoelectric point of $SrTiO_3$ nanoparticle suspension is 3.5.

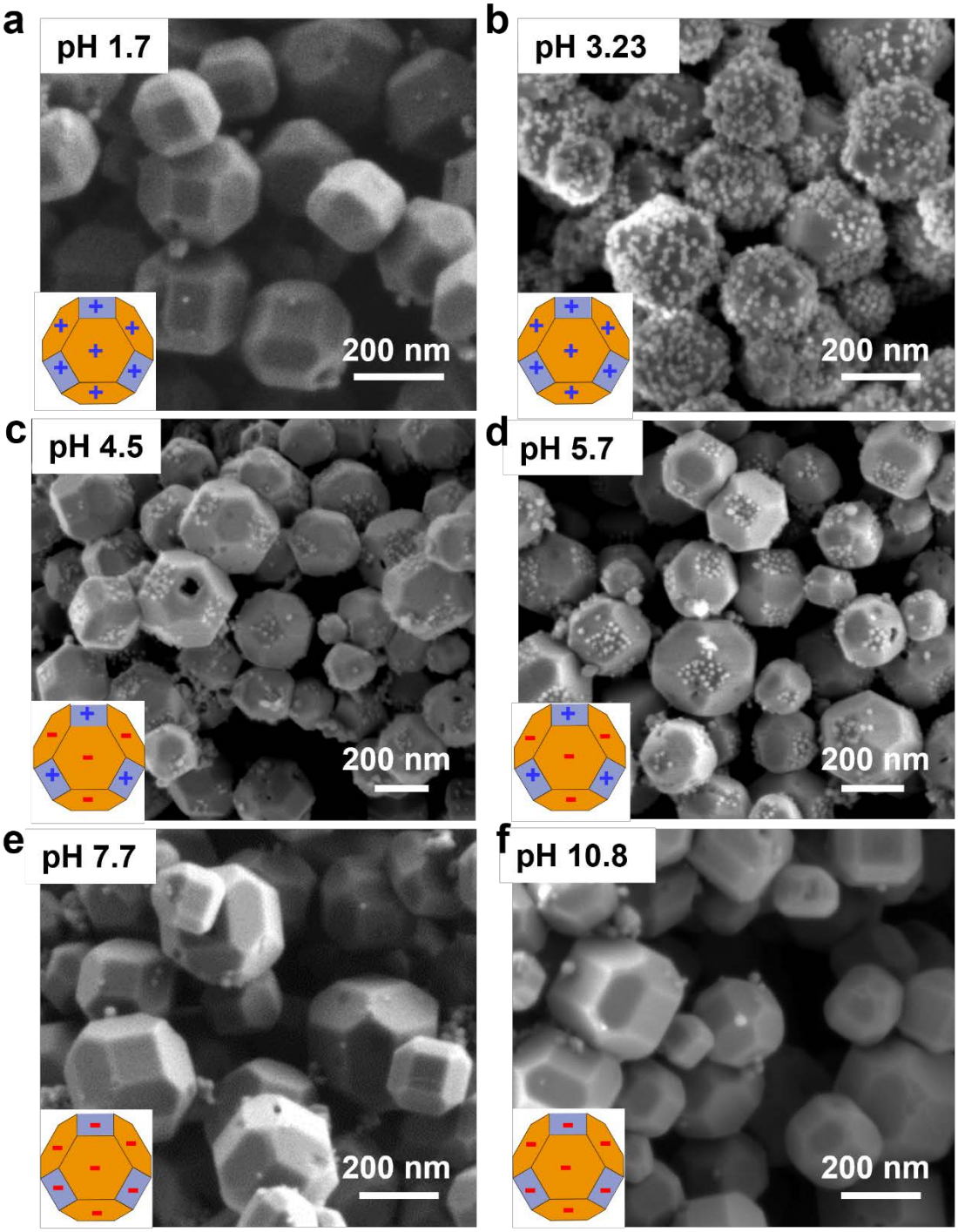

Figure S8. SEM images of $SrTiO_3$ nanoparticle after silica nanoparticles (12 nm) adsorption experiment at different pH. At pH 4 and 5.7 negatively charged SiO2 nanoparticles are adsorbed only on positively charged squared {100} facets. At pH 3.23 both {100} and {110} facets of SrTiO3 are positively charged and negatively charged SiO2 are deposited on both facets. At pH 7.7 and 10.8 negatively charged facets and silica nanoparticles repel each other thus no adsorption of SiO2 particles is observed. At pH 1.7, {100} and {110} facets of SrTiO3 and silica NP are positively charged and hence adsorption is again suppressed for both facets. The insets show the charge sign of individual facets of $SrTiO_3$.

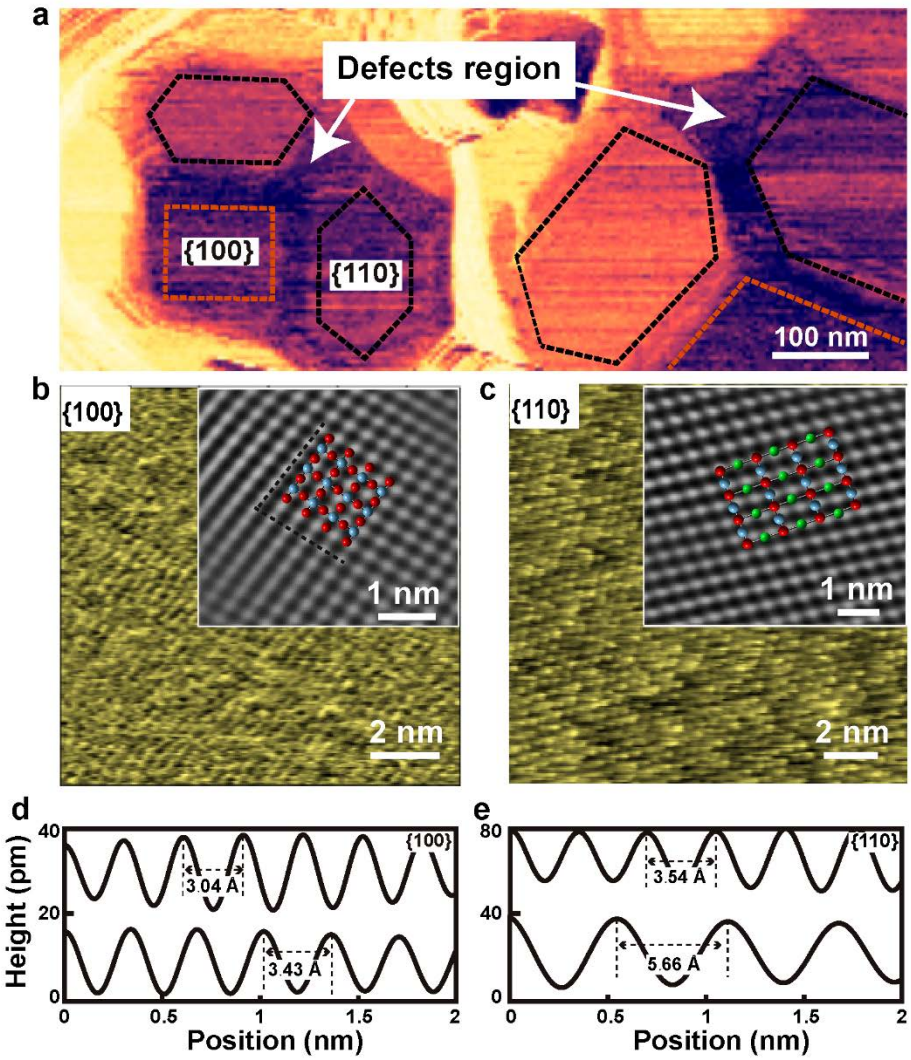

Figure S9. High resolution images on $SrTiO_3$ nanoparticles measured using AM-AFM. a) AFM phase image of $SrTiO_3$ nanoparticles displaying hexagonal {110} and squared {100} facets and also a transition region between several neighbouring facets that display steps and disordered structure. Phase images contrast in regions with defects display a slightly different contrast with respect to the more homogeneous/flat regions, presumably related to variations of local surface chemistry such as a broken bonds. b) Atomic resolution topography images on {100} of $SrTiO_3$ measured in 10 mM NaCl at pH 6. It displays square lattice with lattice parameters a = 0.303 nm and b = 0.343 nm. c) Atomic resolution topography images on {110} facet of $SrTiO_3$ that show a rectangular structure with lattice parameters a = 0.354 nm and b = 0.566 nm. Insets represent Fourier-filtered view of atomic scale images superimposed with X-ray resolved crystallographic structure of {100} and {110}.

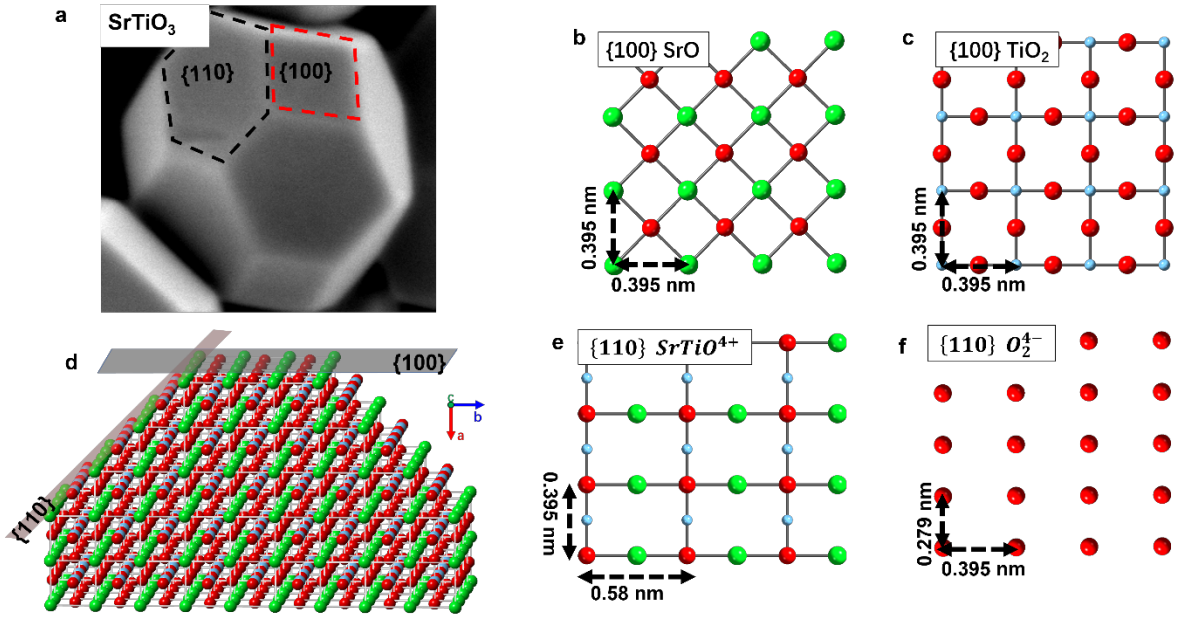

Figure S10. Crystallographic structure of different surface terminations on {100} and {110} facets of $SrTiO_3$. O, Sr and Ti atoms are shown in red, green and blue, respectively. a) SEM image of faceted $SrTiO_3$ nanoparticles with square {100} and hexagonal {110} facets. b, c) The X-ray structure of SrO and TiO_2 terminations of {100} facets displaying a square symmetry with the lattice dimension of 0.395nm. d) 3D crystallographic structure of $SrTiO_3$, emphasizing {100} and {110} planes. e, f) The X-ray structure of $SrTiO^{4+}$ and $(2O)^{4-}$ terminations of {110} facets displaying rectangular structure. The $SrTiO^{4+}$ termination has lattice parameters of 0.395 nm and 0.58 nm between oxygen atoms in two perpendicular directions. For $(2O)^{4-}$ termination, the periodicities are 0.279 nm and 0.395 along the [001] and the [010] directions.

Supplementary Information Note 1

Surface charge determination from force-distance curves: The DLVO-theory with charge regulation is used to extract the surface charge and potential of the $SrTiO_3$ nanoparticles from the measured force distance curves.[1] To do so, we calculate hypothetical force-distance curves for given surface charge and regulation parameter and compare these curves with the measured curves using the surface charge and regulation parameter as fitting parameters.[2][3][4] To determine the force between the tip and particle surface, we first calculate the disjoining pressure $\Pi(h)$ in the gap with height h between them. This pressure can be split in a contribution Π_{vdW} due to van der Waals interactions and an electrostatic double layer contribution Π_{EDL}. The force on the tip is calculated by integrating Π over the spherical tip with radius R_{tip}:

$$F_{int}(h) = \int_h^\infty k_{int}(h')dh' = 2\pi R_{tip}\int_h^\infty [\Pi_{EDL}(h') + \Pi_{vdW}(h')]\,dh' \qquad (1)$$

Ignoring retardation effects, the Van der Waals contribution is calculated using :

$$\Pi_{vdW}(h) = \frac{-A_H}{6\pi h^3} \qquad (2)$$

where A_H is the Hamaker constant, and h is the tip to surface distance. The Hamaker constants A_H for the (silica-water-$SrTiO_3$) system was fixed to $2.259 \cdot 10^{-20}$ J. The electrostatic double layer contribution contains the required information on the surface charge and potential. For a 1-1 electrolyte it is given by:

$$\Pi_{EDL}(h) = c_\infty k_B T\left(4\sinh^2\left(\frac{e\psi(z)}{2k_BT}\right) - \kappa^2\left(\frac{d\psi}{dz}\right)^2\right) \qquad (3)$$

where $\psi(z)$ is the electric potential for $0 < z < h$, k_B being the Boltzmann constant, T the temperature, c_∞ the bulk ion concentration and e the elementary charge; κ is the inverse Debye length:

$$\kappa = \sqrt{\frac{2e^2 C_\infty}{\varepsilon\varepsilon_0 \, k_B T}} \tag{4}$$

Calculation of the electric double layer contribution requires knowledge of the potential $\psi(h)$ in the electrolyte. This potential is governed by the Poisson-Boltzmann (PB) equation:

$$\frac{d^2}{dz^2}\psi(z) = \frac{2e}{\varepsilon\varepsilon_0} \mathrm{c}_\infty \sinh\left(\frac{e\psi(z)}{k_B T}\right) \tag{5}$$

and the boundary conditions at both surfaces. Here we employ the charge regulation (CR) approximation assuming a linear relation between surface charge and surface potential[3]:

$$\sigma_s = \sigma_s^\infty + c_B(\psi_s - \psi_s^\infty) \tag{6}$$

where σ_s^∞ and ψ_s^∞ are the surface charge density and surface potential of the isolated interface, and c_B is an effective capacitance. Here, we refer to surface charge density σ as the charge which is compensating the diffuse layer charge. The surface charge density and surface potential of the isolated interface are related by the Grahame relation:

$$\sigma_s^\infty = 2(2c_\infty \varepsilon\varepsilon_0 \, k_B T)^{1/2} \, \sinh\left(\frac{e\Psi_s^\infty}{2k_b T}\right) \tag{7}$$

When the electrical potential profile $\psi(z)$ is known, the disjoining pressure $\Pi_{EDL}(h, c_B, \psi_s^\infty)$ and the resulting force (or force gradient) are obtained with Equation 3 and 1, respectively. By fitting $\Pi_{EDL}(h, c_B, \psi_s^\infty)$ to the experimentally obtained (h, Π_{EDL}) data, we obtain the desired values for the surface potential ψ_s^∞ and, with Equation 7, the surface charge σ_s^∞. The lower limit for the fitting range is set to 1.5-2 nm, in order to minimize the influence of short range forces, since they are not included in the model. The upper boundary was set to 15 nm, above which the tip–sample interaction force is negligible. Changing the upper limit of the fitting boundary to 20 nm leads to a 1% change in the resulting charge. Variation of the lower limit from 1 to 3.5 nm results in a maximum of 10% change in the surface charge.[2][4]

Supplementary Information Note 2

Surface complexation modeling: The surface charge on solid-water interfaces is modelled using standard surface complexation models involving the adsorption/desorption of ions $X_i \in \{H^+, OH^-, Na^+, Cl^-\}$ to surface sites S according to $\sim SX_i \leftrightarrow \sim S + X_i$. Each reaction is characterized by an equilibrium constant K_i with a corresponding $pK_i = -\log_{10} K_i$. According to the law of mass action, the ion concentration $[X_i]_s$ at the surface depends on the surface concentrations Γ_{SX_i} and Γ_S as: $[X_i]_s = K_i \Gamma_{SX_i}/\Gamma_S$. On the other hand, $[X_i]_s$ is related to the corresponding bulk concentration c_i^∞ by the Boltzmann factor $[X_i]_s = c_i^\infty \exp(-Z_i e\psi_s/k_B T)$, where $Z_i = \pm 1$ is the valency of the ion and ψ_s is the potential at the surface. Moreover, the Grahame equation relates the surface potential to the surface charge: $\sigma_s = 2(2c_\infty \epsilon\epsilon_0 k_B T)^{1/2} \sinh(e\psi_s/2k_B T)$, where c_∞ is the total ionic strength. Using both relations for $[X_i]_s$ the surface charge can be calculated for given I_∞ and pH.[5][6] The experiments have been performed in 10 mM $NaCl$ solutions with different pH values. Since Na^+ and Cl^- weakly absorb on $SrTiO_3$, the surface charge is merely controlled by adsorption or desorption of hydrogen and/or hydroxyl ions. For the O^- terminated [110] facet we assume that the charge of the surface oxygen is compensated by the uptake of a proton:

$$\sim SO^- + H^+ \leftrightarrow \sim SOH\,, \qquad K_1^{[110]} = [H^+]_s \Gamma_{O^-}/\Gamma_{OH} \tag{8}$$

Additional protonation of the surface hydroxyl $\sim SOH$ group yields the formation of $\sim \mathrm{SOH}_2^+$ according to:

$$\sim SOH + H^+ \leftrightarrow \sim \mathrm{SOH}_2^+\,, \quad K_2^{[110]} = [H^+]_s \Gamma_{OH}/\Gamma_{OH_2^+} \tag{9}$$

while $\Gamma_{[110]} = \Gamma_{\mathrm{OH}} + \Gamma_{\mathrm{O}^-} + \Gamma_{OH_2^+}$ is constant. For the TiO_2 terminated [100] facet we assume that the (slightly positive) titanium atom in the interface is able to adsorb a hydroxyl ion while the (slightly negative) oxygen atom can adsorb a proton:

$$\sim STi + OH^- \leftrightarrow \sim STiOH^-, \qquad K_1^{[100]} = [OH^-]_s\, \Gamma_{Ti}/\Gamma_{TiOH^-} \tag{10}$$

$$\sim SO + H^+ \leftrightarrow \sim SOH^+, \qquad K_2^{[100]} = [H^+]_s\, \Gamma_O/\Gamma_{OH^+} \tag{11}$$

while $\Gamma_{[100]} = \Gamma_{Ti} + \Gamma_{TiOH^-} = \frac{1}{2}(\Gamma_O + \Gamma_{OH^+})$ is constant.

The resulting surface charges are given by:

$$\sigma_s^{[110]} = e\Gamma_{[110]}\, \frac{[H^+]_s^2 - K_1^{[110]} K_2^{[110]}}{K_2^{[110]}[H^+]_s + [H^+]_s^2 - K_1^{[110]} K_2^{[110]}}\,, \tag{12}$$

$$\sigma_s^{[100]} = e\Gamma_{[100]} \left(\frac{2[H^+]_s}{K_2^{[100]} + [H^+]_s} - \frac{[OH^-]_s}{K_1^{[100]} + [OH^-]_s} \right) \tag{13}$$

with $[H^+]_s = 10^{-pH} e^{-e\psi_s/k_B T}$ and $[OH^-]_s = 10^{-14}/[H^+]_s$. Substitution of these two expressions in Equation 12 and 13 results in a single implicit equation for σ_s that depends only on the two equilibrium constants K_1 and K_2. Optimal values for K_1 and K_2 (or equivalently pK_1 and pK_2) for both facets can be found by fitting the obtained relation $\sigma_s(pH, K_1, K_2)$ to the experimental (pH, σ_s) data using a least square fit procedure. Parameter values are: $pK_1^{\{100\}} = 5.6$, $pK_2^{\{100\}} = 8.4$, $pK_1^{\{110\}} = 4.3$ and $pK_2^{\{110\}} = 3.1$.

Supplementary References

[1] W. A. Ducker, T. J. Senden, R. M. Pashley, Nature 1991, 353, 239; H.-J. Butt, Biophysical journal 1991, 60, 1438; J. Israelachvili, Intermolecular and surface forces. 2nd ed. Academic Press, London. 1992.

[2] C. Zhao, D. Ebeling, I. Siretanu, D. van den Ende, F. Mugele, Nanoscale 2015, 7, 16298.

[3] F. J. M. Ruiz-Cabello, G. Trefalt, P. Maroni, M. Borkovec, Physical Review E 2014, 90, 012301.

[4] A. Klaassen, F. Liu, D. Van den Ende, F. Mugele, I. Siretanu, Nanoscale 2017, 9, 4721.

[5] T. Hiemstra, J. M. DE WIT, W. Van Riemsdijk, Journal of colloid and interface science 1989, 133, 105.

[6] T. Hiemstra, W. Van Riemsdijk, G. Bolt, Journal of colloid and interface science 1989, 133, 91.